Virology 529 (2019) 144–151

Contents lists available at ScienceDirect

Virology

journal homepage: www.elsevier.com/locate/virology

Identification of virus-encoded circular RNA

Jun-ting Huang[1], Jian-ning Chen[1], Li-ping Gong[1], Yuan-hua Bi, Jing Liang, Lu Zhou, Dan He, Chun-kui Shao*

Department of Pathology, The Third Affiliated Hospital, Sun Yat-sen University, Guangzhou, China

ARTICLE INFO

Keywords:
Epstein-Barr virus (EBV)
Circular RNA
EBV-associated gastric carcinoma
Nasopharyngeal carcinoma
Burkitt lymphoma

ABSTRACT

Circular RNAs (circRNAs) are a novel class of non-coding RNA molecules in eukaryotic organisms that have potentially important roles in gene regulation. Nevertheless, whether viruses can encode circRNA is still uncertain. To examine whether large genome DNA viruses can generate circRNA during the infection of human cells, we performed RNA sequencing of ribosomal RNA-depleted total RNA from Epstein-Barr virus (EBV)-infected cell lines, including SNU-719, AGS-EBV, C666-1 and Akata. We identified an EBV-encoded circRNA, ebv_circ_RPMS1, that consists of the head-to-tail splicing of exons 2–4 from the RPMS1 gene. Furthermore, we demonstrated that ebv_circ_RPMS1 was localized in both cytoplasm and nuclei. Given that circRNAs shape gene expression by titrating microRNAs, regulating transcription and/or interfering with splicing, we identified a novel viral regulator of host and/or viral gene expression.

1. Introduction

Circular RNAs (circRNAs) are covalently closed, single-stranded transcripts that are produced from precursor mRNA (pre-mRNA) back-splicing in eukaryotes (Chen, 2016). Initially, circRNAs were thought to be by-products of splicing errors with few functions (Nigro et al., 1991). Currently, ongoing studies have shown that circRNAs may have potentially important roles in gene regulation, including the titration of microRNAs (miRNAs), regulation of transcription and interference with pre-mRNA splicing (Chen, 2016; Hansen et al., 2013; Kelly et al., 2015; Memczak et al., 2013). Next-generation RNA sequencing (RNA-seq) of non-polyadenylated transcriptomes has recently shown that the expression of circRNAs is ubiquitous (Broadbent et al., 2015; Chen, 2016; Lu et al., 2015; Wang et al., 2014). Over ten thousand different circRNAs have been successfully identified in metazoans, from fruit flies and worms to mice and humans (Chen, 2016; Wang et al., 2014). Furthermore, circRNAs have been found in plants, fungi and protists (Broadbent et al., 2015; Lu et al., 2015; Wang et al., 2014). Nevertheless, whether viruses generate circRNAs remains unknown.

Epstein-Barr virus (EBV) is a large genomic DNA virus of the herpesvirus family that infects over 90% of adults worldwide (Young et al., 2016). EBV is causally associated with a number of lymphoid and epithelial malignancies, including Burkitt lymphoma (BL), Hodgkin lymphoma (HL), certain subtypes of non-Hodgkin lymphoma (both B- and T-cell lymphomas), post-transplant lymphoproliferative disease (PTLD), nasopharyngeal carcinoma (NPC) and a subset (~ 10%) of gastric carcinomas defined as EBV-associated gastric carcinomas (EBVaGCs) (Rickinson and Kieff, 2007; Young et al., 2016). An estimated 143,000 deaths worldwide in 2010 were attributed to these EBV-associated malignancies, representing 1.8% of all cancer deaths (Khan and Hashim, 2014). Furthermore, EBV can cause lymphoproliferative phenotypes, ranging from common infectious mononucleosis (IM) to rare hemophagocytic lymphohistiocytosis (Taylor et al., 2015). Additionally, EBV presents as chronic active infections (Fujiwara et al., 2014) and is associated with autoimmune disorders such as multiple sclerosis (MS) (Pohl et al., 2006). The genome of EBV is approximately 170 kb, encoding more than 80 proteins (Rickinson and Kieff, 2007). In addition, EBV also produces non-coding RNAs (ncRNAs), including EBV-encoded small RNAs (EBERs), miRNAs and long non-coding RNAs (lncRNAs) (Marquitz et al., 2015; Pfeffer et al., 2004; Rickinson and Kieff, 2007). Nevertheless, it remains uncertain as to whether EBV encodes circRNA. Some EBV transcripts, including latent membrane protein 1 (LMP1), LMP2 and *Bam*HI-A rightward transcripts (BARTs), contain both exons and introns. Theoretically, it is possible that EBV could generate circRNA.

To investigate whether EBV encodes circRNA, we performed RNA-seq analysis of ribosomal RNA-depleted total RNA from EBV-infected cell lines SNU-719, AGS-EBV, Akata and C666-1. We found that there were EBV-derived back-spliced circRNA reads that were further confirmed as EBV-encoded circRNAs. In addition, we investigated the

* Correspondence to: The Third Affiliated Hospital, Sun Yat-sen University, China.
E-mail address: shaochk@mail.sysu.edu.cn (C.-k. Shao).
[1] These authors contributed equally to this work.

https://doi.org/10.1016/j.virol.2019.01.014
Received 28 August 2018; Received in revised form 11 January 2019; Accepted 14 January 2019
Available online 16 January 2019

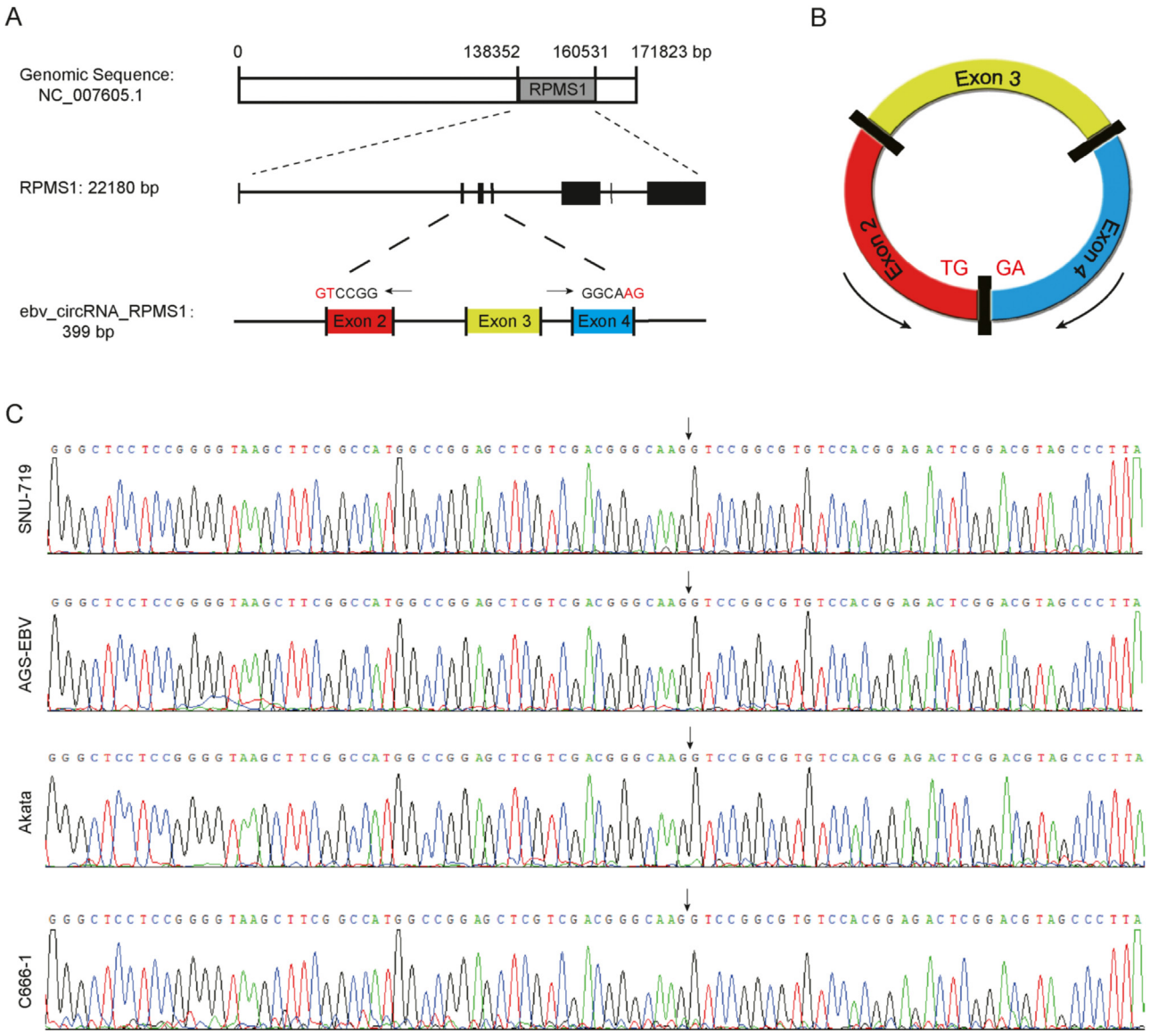

Fig. 1. Schematic illustration of ebv-circRPMS1. (A) Genomic location of the RPMS1 gene and ebv-circRPMS1. (B) Schematic illustration showing the circularization of RPMS1 exons 2–4 forming ebv-circRPMS1. (C) The existence of ebv-circRPMS1 was validated by RT-PCR and DNA sequencing. Arrow represents "head-to-tail" splicing sites of ebv-circRPMS1.

expression of these ebv-circRNAs in both cell lines and tumor tissues. Finally, the possible functions of these ebv-circRNAs were explored.

2. Results and discussion

In the present study, we performed RNA-seq analysis of ribosomal RNA-depleted total RNA from EBV-infected cell lines SNU-719 (latency I), AGS-EBV (latency I), Akata (latency I) and C666-1 (latency II). We found that there were EBV-derived back-spliced circRNA reads, whose sequences were mapped to the reference EBV genomic sequence (NC_007605.1) by NCBI Blast (S1 Table). This candidate circRNA consisted of the head-to-tail splicing of exons 2–4 from the RPMS1 gene (399 bp) (Fig. 1A, B and S1 Appendix). We called this circRNA ebv_circRNA_RPMS1 (ebv-circRPMS1). RPMS1 is located within the EBV *Bam*HI-A rightward transcripts (BARTs) region and has been shown to have some biochemical functions relevant to tumorigenesis (Li et al., 2005). Exons 2–4 of RPMS1 are flanked by long introns on each side, containing reverse complementary sequences that may ease the circularization of RNA to form circRNA. RT-PCR using divergent primers (outward-facing primers) and following DNA sequencing confirmed the head-to-tail splicing product of the expected size (Fig. 1C).

According to previously described methodology (Jeck and Sharpless, 2014), we designed both convergent primers and divergent primers to amplify RPMS1 mRNA and ebv-circRPMS1 in EBV-positive cell lines (SNU-719, AGS-EBV, C666-1, Akata and B95.8) and EBV-negative AGS cell lines (Fig. 2A). Ebv-circRPMS1 was only amplified by divergent primers in cDNA of SNU-719, AGS-EBV, C666-1, and Akata but not in cDNA of AGS and B95.8, which harbors a deletion in this RPMS1 locus. In addition, no amplification product was observed in the genomic DNA (gDNA) of all cell lines tested (Fig. 2B). RT-PCR using the divergent primers of ebv-circRPMS1 and the total RNA treated with RNase R exonuclease as a template also amplified ebv-circRPMS1, indicating that the total RNA contained RNA existing in circular form without a polyadenylated tail (ebv-circRPMS1) that was resistant to digestion by RNase R exonuclease (Fig. 2C). The relative abundance of ebv-circRPMS1 and RPMS1 mRNA in EBV-positive cell lines SNU-719, Akata and C666-1 is shown in S1 Figure. BaseScope assays performed on EBVaGC cell lines SNU-719 and AGS-EBV (latency I), SNU-719 xenografts (latency I) and EBVaGC tissues (latency I) as well as EBV-positive NPC cell line C666-1 (latency II) and NPC tissues (latency II)

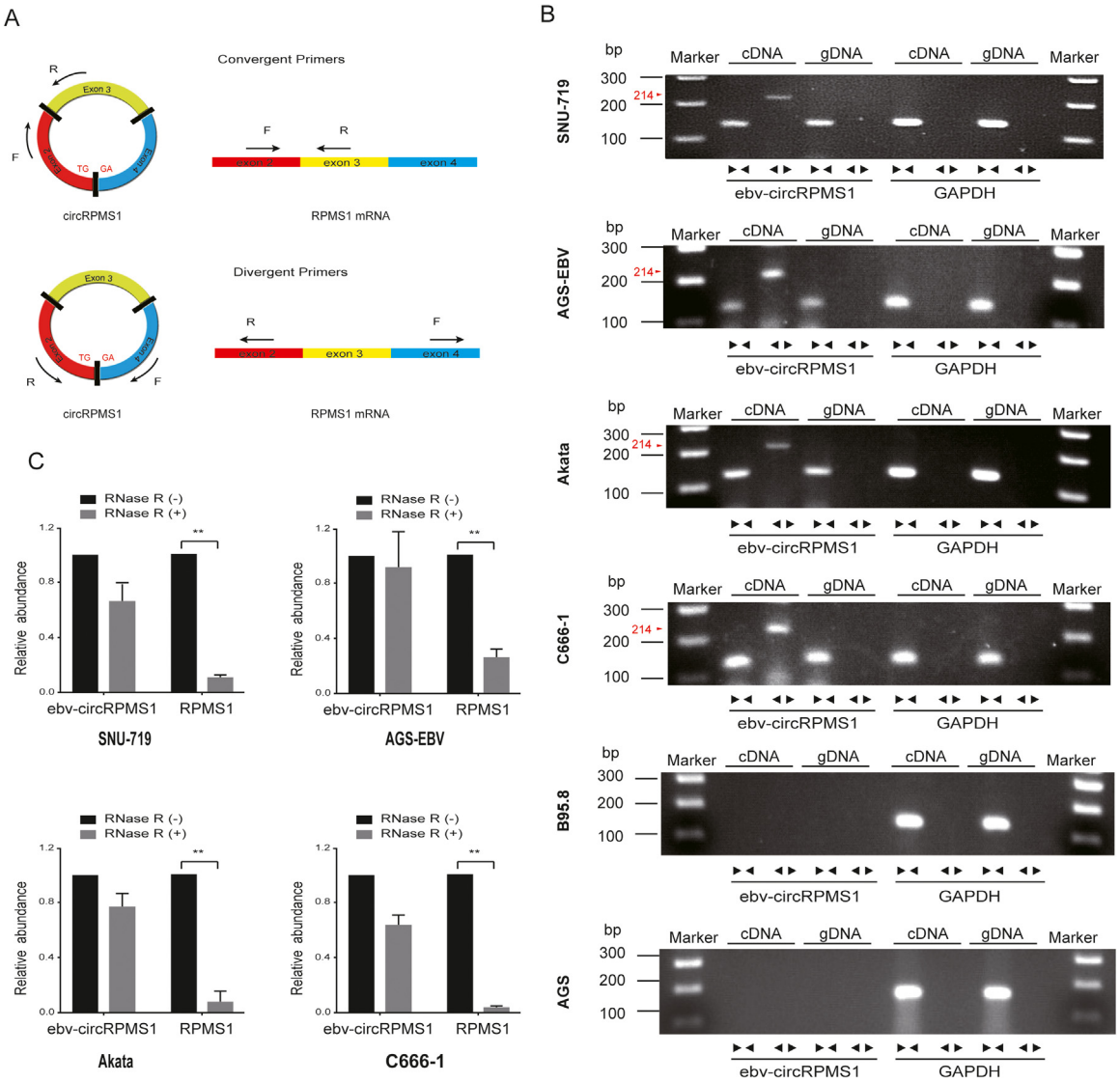

Fig. 2. Expression of ebv-circRPMS1 in EBV-infected cell lines. (A) Schematic diagram of divergent and convergent primers. Divergent primers amplified ebv-circRPMS1 but not RPMS1 mRNA, while convergent primers amplified both. (B) Ebv-circRPMS1 was expressed in EBV-positive SNU-719, AGS-EBV, Akata and C666-1 cells, but not in AGS and B95.8 cells. Divergent primers amplified ebv-circRPMS1 cDNA (214 bp, red arrow head) but not RPMS1 genomic DNA (gDNA), while convergent primers amplified both ebv-circRPMS1 cDNA and RPMS1 gDNA. GAPDH was used as a negative control for circRNA. (C) The expression of ebv-circRPMS1 and RPMS1 mRNA in EBV-positive SNU-719, AGS-EBV, Akata and C666-1 cells treated with or without RNase R was detected by RT-PCR. After RNase R digestion, the expression of RPMS1 mRNA reduced remarkably, while that of ebv-circRPMS1 was not significantly reduced, suggesting that ebv-circRPMS1 was resistant to RNase R. Data are expressed as the mean ± SD, n = 3. **p < 0.01 (Student's *t*-test).

demonstrated that ebv-circRPMS1 localized both in cytoplasm andnuclei (Fig. 3A, B). qRT-PCR analysis of nuclear and cytoplasmic RNAs also showed that ebv-circRPMS1 existed both in cytoplasm and nuclei, while its cognate RPMS1 mRNA was primarily localized within the nuclei (Fig. 3C). It has been shown that the BART transcripts (including RMPS1 and BARF0) were expressed extensively only in the nucleus but not in the cytoplasm, arguing against their role as mRNAs (Jang et al., 2011). Here, we showed that, although RPMS1 mRNA was primarily localized within the nuclei, ebv-circRPMS1, which is another RNA that is also derived from the same pre-mRNA, localized in both cytoplasm andnuclei.

Given that cytoplasmic circRNA usually functions as a miRNA sponge in RNA-guided gene regulation, we wondered whether ebv-circRPMS1 could function as a miRNA sponge in the cytoplasm. Therefore, the bioinformatic databases RegRNA2.0 (Chang et al., 2013) and RNAhybrid (Rehmsmeier et al., 2004) were used to identify targets for ebv-circRPMS1. As shown in S2 Table and Table 1, we found 47 candidate human miRNAs and 8 candidate EBV miRNAs as targets of ebv-circRPMS1 by overlapping the prediction results of both programs. Some of these miRNAs have been reported to target and regulate the expression of certain genes. For example, hsa-miR-28-5p was found to be a tumor suppressor targeting RAP1B in renal cell carcinoma (Wang et al., 2016) and insulin-like growth factor-1 (IGF-1) in hepatocellular carcinoma (Shi and Teng, 2015). Ebv-miR-BART20-5p was suggested to directly suppress the expression of both BZLF1 and BRLF1 to maintain EBVaGC latency (Jung et al., 2014). Specially, ebv-miR-BART13-5p was predicted to have 3 binding sites of circRPMS1 (Table 1). These findings suggested that ebv-circRPMS1 likely serves as a miRNA sponge, bounded by both human and EBV miRNAs and sequestering miRNAs from their targets, thus regulating the expression of other genes. To further test this hypothesis, an ebv-circRPMS1 over-expression plasmid was constructed and transfected into EBV-negative AGS cells (Fig. 4A). Consistent with the prediction results by bioinformatics method, 11 of 14 human miRNAs were downregulated significantly by ebv-circRPMS1

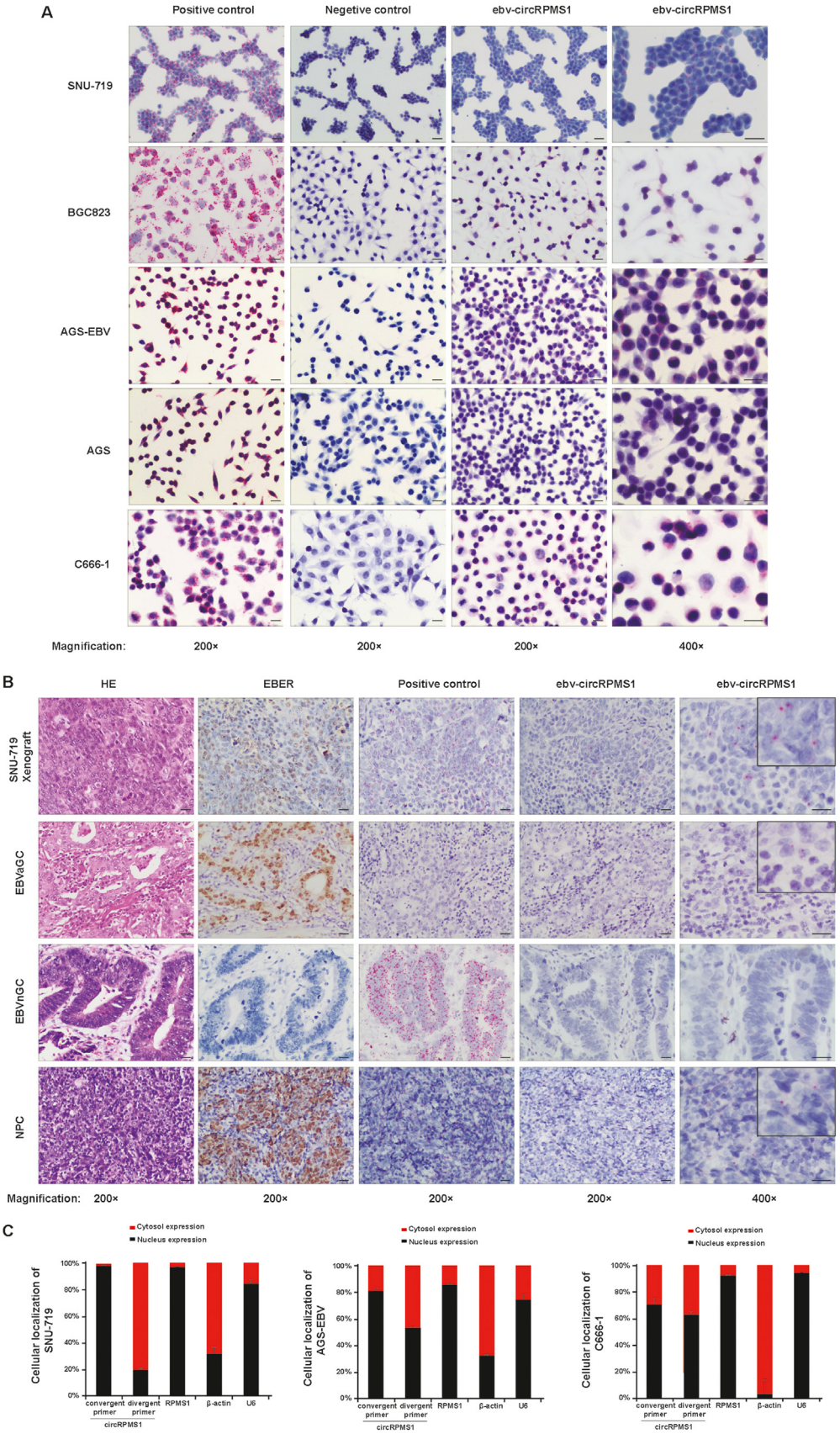

Fig. 3. Ebv-circRPMS1 was localized both in cytoplasm and nuclei. (A) BaseScope detection of ebv-circRPMS1 in EBV-positive cells (SNU-719, AGS-EBV and C666-1) and EBV-negative cells (AGS and BGC823). Positive signals (red) were observed in the cytoplasm and nuclei of EBV-positive cells but not in EBV-negative cells. Nuclei were counterstained with hematoxylin. Scale bars, 20 μm. (B) BaseScope detection of ebv-circRPMS1 in SNU-719 xenograft and human carcinoma tissues. Positive signals were observed in SNU-719 xenograft, human EBVaGC tissue and NPC tissue, while no signals were detected in EBVnGC tissue. The location of the red dot signals was in the cytoplasm and the nuclei. Scale bars, 20 μm. (C) The subcellular localization of ebv-circRPMS1 in EBV-positive SNU-719, AGS-EBV and C666-1cells. After nuclear and cytoplasmic fraction separation, RNA expression levels were measured by qRT-PCR. β-actin was used as a cytoplasmic marker and U6 was used as a nuclear marker. Ebv-circRPMS1 was localized both in the cytoplasm and nuclei of the EBV-infected cells.

(Fig. 4B). In addition, wound healing assays showed that the migration of cells in the AGS-cicRPMS1 group was faster than that in the AGS group and AGS-NC group (Fig. 4C). Although the molecular mechanisms behind this phenomenon are still unexplored, these preliminary results provided some justification supporting that ebv-circRPMS1 may act as a miRNA sponge.

Table 1
Examples of predicted EBV miRNA-binding sites of circRPMS1.

EBV miRNA	Position[a]	Minimum free energy (kcal/mol)[b]	Score[b]	Alignment (miRNA top row 3′-5′)
ebv-miR-BHRF1-1	252–274	− 20.53	116.00	Query: 3′ uuGA-GGCCCCGACUAGUCCAAu 5′ || ||| | ||: ||: ||| Ref: 5′ ggCTGCCGTAGGTGGTCGTGTTg 3′
ebv-miR-BART3-3p	325–346	− 23.06	136.00	Query: 3′ ugUGGACCACUGAUCACCACGc 5′ :|| || : ||||| ||| Ref: 5′ gcGCCGGGACGCTAGTGCTGCa 3′
ebv-miR-BART4-3p	247–271	− 22.19	117.00	Query: 3′ ugUGGACCACGG-AUGCACUA-CAc 5′ | | | |||| || |||: | || Ref: 5′ gtAGCGGCTGCCGTAGGTGGTCGTg 3′
ebv-miR-BART10-5p	246–267	− 21.18	120.00	Query: 3′ aCAU-GUCU-UGGUUUCUCCACCg 5′ ||| |: | : ||: ||||| Ref: 5′ aGTAGCGGCTGCCGT–AGGTGGt 3′
ebv-miR-BART12	59–77	− 22.72	108.00	Query: 3′ uugGUGUGGUUUGUGGUGUCCu 5′ |||||| : || |: || Ref: 5′ ggaCACACC—TTCCCCGGGa 3′
ebv-miR-BART13-5p	359–383	− 26.22	121.00	Query: 3′ gaCAUGC——UCGGUGCUCGGCCaa 5′ ||| | : ||||: : |||| Ref: 5′ ggGTAAGCTTCGGCCAT-GGCCGGag 3′
ebv-miR-BART13-5p	283–303	− 22.70	109.00	Query: 3′ gacaUGCUCGGUGCUCGGCCaa 5′ ::|: |||:| || ||| Ref: 5′ agaaGTGGGCCGC-AGGCGGcg 3′
ebv-miR-BART13-5p	314–333	− 20.45	108.00	Query: 3′ gaCAUGCUCGGUGCUCGGCCaa 5′ | |||| |: | |||| Ref: 5′ ctGAACGA–CGAGCGCCGGga 3′
ebv-miR-BART14-5p	241–266	− 23.10	126.00	Query: 3′ acAUUU-A–GCCGUC-GCAUCCcau 5′ |||| | |||| | ||||| Ref: 5′ cgTAAAGTAGCGGCTGCCGTAGGtgg 3′
ebv-miR-BART20-5p	105–123	− 20.75	115.00	Query: 3′ ccUUACUUCUGUACGGACGAu 5′ ||||::|: | |: |||| Ref: 5′ gaAATGGGGGC–GTGTGCTg 3′

[a] The position is indicated relative to the sequence of ebv-circRPMS1.
[b] The minimum free energy and scores were obtained from RegRNA 2.0.

In addition to being a cytoplasmic circRNA, ebv-circRPMS1 is also localized in nuclei. It has been reported that nuclear circRNA regulated gene transcription via specific RNA-RNA interaction (Li et al., 2015; Zhang et al., 2013). Thus, it might also be possible that ebv-circRPMS1 functions as a gene transcription regulator that ultimately affects gene expression.

While our manuscript was under review, two more comprehensive reports on ebv-circRNAs have been published (Toptan et al., 2018; Ungerleider et al., 2018). Both reports found that EBV could encode circRNAs, which included ebv-circRPMS1 (also called ebv-circBARTs in Toptan et al.'s study), ebv-circLMP2 and ebv-circBHLF1. Ebv-circRPMS1 was found to be expressed in EBV-positive cell lines and tissues representing latency types I, II, and III, including EBV-positive PTLD, BL, EBVaGC, NPC, and AIDS-associated lymphoma (Toptan et al., 2018; Ungerleider et al., 2018). Besides, ebv-circRPMS1 was also found to be expressed during reactivation (Ungerleider et al., 2018). In addition to EBV, Kaposi's sarcoma herpesvirus (KSHV) can also generate circRNAs (Toptan et al., 2018). However, both studies did not explore the functions of EBV-encoded circRNAs. In the present study, we made some preliminary exploration regarding the possible function of ebv-circRPMS1; and our results suggested that ebv-circRPMS1 could act as a miRNA sponge.

In summary, our study identified an EBV-encoded circRNA, ebv-circRPMS1, and showed that ebv-circRPMS1 localized both in cytoplasm and nuclei, where it might have potential functions. These findings suggest that EBV, and probably other Herpesvirus and large genome DNA viruses, encode circRNAs, possibly serving as a strategy for the regulation of host and viral gene expression and thus playing important roles in the host-virus interaction.

3. Materials and methods

3.1. Cell lines

The cell lines used in the present study included EBV-negative gastric cell lines AGS and BGC823, EBV-positive gastric cell lines SNU-719 and AGS-EBV, EBV-positive NPC cell lines C666-1 and EBV-positive BL cell line Akata. AGS artificially infected with a recombinant EBV using the cell-to-cell contact method was adopted to construct EBV-infected AGS cell line (AGS-EBV) (Imai et al., 1998). The BL cell line Akata was modified to produce recombinant EBV, in which a neomycin resistance gene (Neo^r) was inserted into the BXLF1 site of EBV DNA; this virus was used in the present study.

All cells were cultured in RPMI-1640 medium (Gibco, USA) supplemented with 10% fetal bovine serum (FBS; Gibco) and maintained in a humidified atmosphere with 5% CO_2 at 37 °C. AGS-EBV cells were also maintained with 500 μg/mL G418 (Gibco) to select for retention of the EBV episome.

3.2. Xenograft and human tissue specimens

The NOD/SCID mice (female, 4–6 weeks old; Model Animal Research Center of Nanjing University, Nanjing, China) were subcutaneously implanted with 2×10^6 cells of SNU-719 into the dorsum next to the right hind leg. After 4 weeks, the mice were sacrificed, and the SNU-719 xenografts were obtained. Formalin-fixed, paraffin-embedded tissue specimens of primary EBVaGC (10 cases), EBVnGC (10 cases) and NPC (10 cases) were obtained from the patients who underwent surgeries at The Third Affiliated Hospital, Sun Yat-sen University, Guangzhou, China. EBV-encoded small RNA 1 (EBER-1) *in*

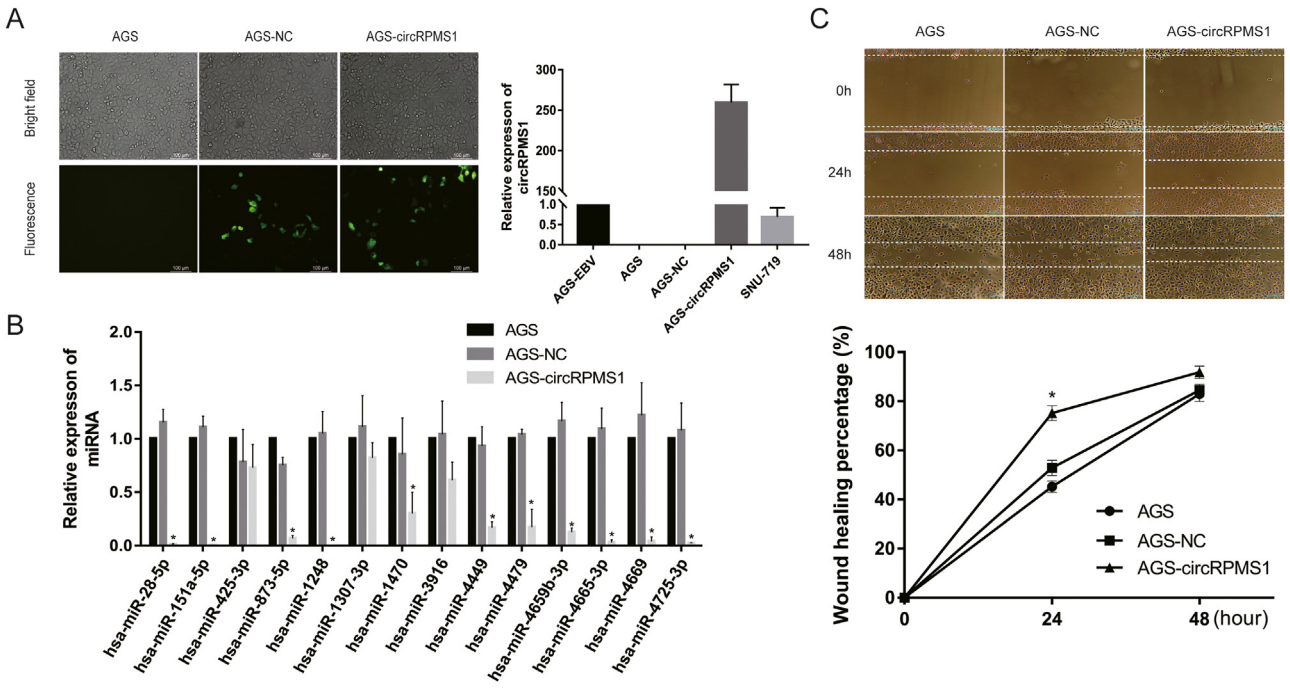

Fig. 4. Ebv-circRPMS1 downregulated human miRNA expression and promoted cell migration. (A) Transfection of ebv-circRPMS1 over-expression plasmid. The pcD25-ciR vector contained GFP protein which can be observed under fluorescence microscope. The relative expression levels of ebv-circRPMS1 were detected by qRT-PCR. Ebv-circRPMS1 was highly expressed in AGS cells after transfection of ebv-circRPMS1 over-expression plasmid (AGS-circRPMS1). AGS-EBV and SNU-719 cells were served as positive controls, while AGS cells were used as negative control. (B) Relative expression of several human miRNAs before and after ebv-circRPMS1 over-expression. Eleven of 14 human miRNAs were downregulated significantly by ebv-circRPMS1. (C) The effect of ebv-circRPMS1 on cell migration capability was evaluated by wound healing assay. The migration of cells in the AGS-circRPMS1 group was significantly faster than that in the AGS group and AGS-NC group. Data are expressed as the mean ± SD, n = 3. *P < 0.05. Scale bar, 100 μm.

situ hybridization assay was performed to confirm EBV infection. Informed consents were obtained from all patients and ethical guidelines under Declaration of Helsinki were followed. The research protocol was approved by the Experimental Animal Ethics Committee and the Clinical Research Ethics Committee of the Third Affiliated Hospital, Sun Yat-sen University.

3.3. RNA sequencing (RNA-seq)

Total RNA was extracted from cultured cells using TRIzol reagent (Invitrogen, Carlsbad, CA, USA). Approximately 3 μg of the total RNA was subjected to the RiboMinus Eukaryote Kit (Qiagen, Valencia, CA, USA) to remove ribosomal RNA prior to the construction of the RNA-seq libraries. Strand-specific RNA-seq libraries were prepared using the NEBNext Ultra Directional RNA Library Prep Kit for Illumina (NEB, Beverly, MA, USA). Briefly, approximately 50 ng of the ribosome-depleted RNA samples was fragmented and then used for first- and second-strand cDNA synthesis with random hexamer primers. A dUTP mix was used for second-strand cDNA synthesis. An End-It DNA End Repair Kit was used to repair the ends of the double stranded cDNA fragments, which were then modified by the Klenow fragment such that an A was added to the 3′-end of the DNA fragments and were finally ligated to adapters. The ligated products were purified and treated with uracil DNA glycosylase (UDG) to remove the second-strand cDNA. Purified first-strand cDNA was subjected to 13–15 cycles of PCR amplification, followed by analysis of the libraries with a Bioanalyzer 2100 (Agilent, Santa Clara, CA, USA); the cDNA was then sequenced in a HiSeq. 2000 system (Illumina, San Diego, CA, USA) on a 100-bp paired-end run.

3.4. Identification and annotation of circRNA

The reference human genome (GRCh38/hg38) was obtained from the UCSC genome browser (http://genome.ucsc.edu/), and the reference EBV genome (Accession No. NC_007605.1) was obtained from NCBI GenBank (http://www.ncbi.nlm.nih.gov/). First, FASTQ reads that aligned contiguously and full-length to the genomes by TopHat2 (Kim et al., 2013) were discarded. Next, from the unmapped reads, we extracted 20-nt from both ends and aligned them independently to find unique anchor positions within spliced exons by TopHat2 again. Anchors that aligned in the reverse orientation (head-to-tail) represent a back-spliced junction. Anchor alignments were extended such that the complete read alignments and the breakpoints were flanked by a GT/AG splice site. We mapped the splicing ends of each circRNA to the genomic regions and then compared the results to the RefSeq and NCBI databases to annotate the functional element of circRNA. We searched for the longest transcript fragment whose boundaries (5′-end or 3′-end) exactly matched both ends of this circRNA in the same strand and then defined the corresponding gene of this transcript fragment as the cognate gene of this circRNA.

3.5. RNA preparation, RNase R treatment, RT-PCR and DNA Sequencing

Total RNA was extracted from cultured cells using TRIzol reagent (Invitrogen, Carlsbad, CA, USA) according to the manufacturer's instructions. For RNase R treatment, 2 μg of total RNA was incubated with 3 U/μg of Rnase R (Epicenter Technologies, Madison, WI, USA) for 15 min at 37 °C. For subcellular localization studies, the nuclear and cytoplasmic fractions were separated using the Nuclear/Cytosol Fractionation Kit (BioVision, CA, USA) according to the manufacturer's instructions.

To quantify the amount of mRNA and circRNA, cDNA was synthesized using a Reverse Transcription Kit (Takara,Dalian, China) according to the manufacturer's instructions. To quantify the amount of mature miRNA, Mir-X™ miRNA First Strand Synthesis Kit (Takara, Dalian, China) was used. Then, real-time quantitative reverse

transcription-polymerase chain reaction (RT-PCR) analyses were performed on an ABI 7500 FAST Real-Time PCR System (Applied Biosystems, Carlsbad, CA, USA) using SYBR® *Premix Ex Taq*™ II Kit (Takara, Dalian, China). The comparative C_T (cycle threshold) method was used to calculate the relative expression of different RNA. Glyceraldehyde 3-phosphate dehydrogenase (GAPDH) and U6 were used as internal controls. The primers used in the present study are listed in Table S3. The resultant PCR products were visualized by electrophoresis in a 1.5% agarose gelstained with 0.5 mg/mL of ethidium bromide and photographed under UV light. Some PCR products were also subjected to DNA sequencing. Cycle sequencing was carried out on 3730xl DNA Analyzers using the ABI PRISM Big Dye Terminator Cycle Sequencing Ready Reaction Kit (PE Applied Biosystems, Foster City, CA) according to the manufacturer's manual. All sequences were sequenced bi-directionally.

3.6. BaseScope in situ hybridization

BaseScope assays were performed according to the manufacturer's instructions (Advanced Cell Diagnostics, Inc., Newark, CA, USA). Briefly, the cell or tissue sections were baked for 1 h at 60 °C, deparaffinized, and treated with pretreat solution for 10 min at room temperature. Target retrieval was performed for 15 min at 100 °C, followed by protease treatment for 15 min at 40 °C. Probes were then hybridized for 2 h at 40 °C followed by BaseScope amplification and fast red chromogenic detection. BaseScope probe design has been previously described (Wang et al., 2012). The following BaseScope probes were used in this study: positive control probe against the human endogenous housekeeping gene peptidyl prolyl isomerase B (Hs-PPIB), negative control probe against bacterial gene dihydrodipicolinate reductase (dapB), and target probe against ebv-circRPMS1 (the probe sequences are available upon request). All the probes were designed and synthesized by Advanced Cell Diagnostics, Inc. (USA). The images were acquired on an Olympus Microscope (Olympus, Japan).

3.7. ebv-circRPMS1 target prediction

Prediction of the miRNA-binding sites of ebv-circRPMS1 was performed using the bioinformatic databases RegRNA (v2.0, http://regrna2.mbc.nctu.edu.tw/) (Chang et al., 2013) and RNAhybrid (http://bibiserv.techfak.uni-bielefeld.de/rnahybrid/) (Rehmsmeier et al., 2004). For RegRNA, the filtering restrictions were as follows: (i) minimum free energy (MFE) ≤ -20 kcal/mol; (ii) Score ≥ 140 for hsa-miRNAs or Score ≥ 100 for ebv-miRNAs. For RNAhybrid, we first obtained the sequences of 2656 mature human miRNAs and 44 mature EBV miRNAs from miRBase (http://www.mirbase.org/, Release22, March 2018) (Kozomara and Griffiths-Jones, 2014). Then, algorithms from RNAhybrid was adopted with the following filtering restrictions: (i) minimum free energy (MFE) ≤ -20 kcal/mol; (ii) hits per target ≤ 3. Targets that were overlapped by both predictions were selected as candidate miRNA-binding sites of ebv-circRPMS1.

3.8. CircRNA plasmid construction and transfection

To construct ebv-circRPMS1 over-expression plasmid, the ebv-circRPMS1 cDNA was amplified using KOD Plus Neo (TOYOBO, Japan). The PCR products were then inserted into a pCD25-ciRvector (Geenseed Biotech Co., Guangzhou, China). The pcD25-ciR vector contained a front circular frame and a back circular frame. Transfection was carried out using Lipofectamine 3000 (LifeTechnologies, USA) according to the manufacturer's instructions. The constructs were verified by Sanger sequencing.

3.9. Wound healing assay

Cells were cultured in six-well plates and scraped with fine end of 200 μL pipette tips (time 0 h). Cell migration was photographed using 10 high-power fields at 0, 24 and 48 h after injury. Remodeling was measured as diminishing distance across the induced injury, normalized to the 0 h control and expressed as relative migration.

3.10. Statistical analysis

All data are representative of three independent experiments. The data are expressed as the mean ± SD. The results were considered statistically significant at a *p*-value of less than 0.05 using Student's *t*-test (two-tailed). All statistical analyses were performed using SPSS20.0 software (IBM, SPSS, USA).

Acknowledgements

This work was supported by the National Natural Science Foundation of China (Nos. 81572309 & 81272553 to C.K.S., No. 81301694 to J.N.C.), the Natural Science Foundation of Guangdong Province (Nos. 2017A030313502 & 2014A030313034 to C.K.S.) and the Guangzhou Science and Technology Project (No. 201707010119 to C.K.S.), Guangdong Province, China.

Data and materials availability

All data is available in the main text or in the Supporting information.

Conflicts of interest

None.

Funding

This work was supported by the National Natural Science Foundation of China (Nos. 81572309 & 81272553 to C.K.S., No. 81301694 to J.N.C.), the Natural Science Foundation of Guangdong Province (Nos. 2017A030313502 & 2014A030313034 to C.K.S.) and the Guangzhou Science and Technology Project (No. 201707010119 to C.K.S.), Guangdong Province, China.

Author summary

Circular RNAs (circRNAs) are a novel class of non-coding RNAs that have gained increasing attention in recent years. These circRNAs have been identified in humans, mice, worms, fruit flies, plants, fungi and protists. Nevertheless, it remains unknown whether viruses generate circRNAs. To examine whether large genome DNA viruses encode circRNA, we performed RNA sequencing of ribosomal RNA-depleted total RNA from EBV-infected cell lines and identified an EBV encoded circRNA, ebv_circ_RPMS1. Since circRNAs may have potentially important roles in gene regulation, our findings shed light on a new research field regarding host-virus interactions.

Appendix A. Supplementary material

Supplementary data associated with this article can be found in the online version at doi:10.1016/j.virol.2019.01.014.

References

Broadbent, K.M., Broadbent, J.C., Ribacke, U., Wirth, D., Rinn, J.L., Sabeti, P.C., 2015. Strand-specific RNA sequencing in Plasmodium falciparum malaria identifies developmentally regulated long non-coding RNA and circular RNA. BMC Genom. 16, 454.

Chang, T.H., Huang, H.Y., Hsu, J.B., Weng, S.L., Horng, J.T., Huang, H.D., 2013. An enhanced computational platform for investigating the roles of regulatory RNA and for identifying functional RNA motifs. BMC Bioinforma. 14 (Suppl. 2), S4.

Chen, L.L., 2016. The biogenesis and emerging roles of circular RNAs. Nat. Rev. Mol. Cell

Biol. 17, 205–211.
Fujiwara, S., Kimura, H., Imadome, K., Arai, A., Kodama, E., Morio, T., Shimizu, N., Wakiguchi, H., 2014. Current research on chronic active Epstein-Barr virus infection in Japan. Pediatr. Int. 56, 159–166.
Hansen, T.B., Jensen, T.I., Clausen, B.H., Bramsen, J.B., Finsen, B., Damgaard, C.K., Kjems, J., 2013. Natural RNA circles function as efficient microRNA sponges. Nature 495, 384–388.
Imai, S., Nishikawa, J., Takada, K., 1998. Cell-to-cell contact as an efficient mode of Epstein-Barr virus infection of diverse human epithelial cells. J. Virol. 72, 4371–4378.
Jang, B.G., Jung, E.J., Kim, W.H., 2011. Expression of *Bam*HI-A rightward transcripts in Epstein-Barr virus-associated gastric cancers. Cancer Res. Treat. 43, 250–254.
Jeck, W.R., Sharpless, N.E., 2014. Detecting and characterizing circular RNAs. Nat. Biotechnol. 32, 453–461.
Jung, Y.J., Choi, H., Kim, H., Lee, S.K., 2014. MicroRNA miR-BART20-5p stabilizes Epstein-Barr virus latency by directly targeting BZLF1 and BRLF1. J. Virol. 88, 9027–9037.
Kelly, S., Greenman, C., Cook, P.R., Papantonis, A., 2015. Exon skipping is correlated with exon circularization. J. Mol. Biol. 427, 2414–2417.
Khan, G., Hashim, M.J., 2014. Global burden of deaths from Epstein-Barr virus attributable malignancies 1990–2010. Infect. Agent Cancer 9, 38.
Kim, D., Pertea, G., Trapnell, C., Pimentel, H., Kelley, R., Salzberg, S.L., 2013. TopHat2: accurate alignment of transcriptomes in the presence of insertions, deletions and gene fusions. Genome Biol. 14, R36.
Kozomara, A., Griffiths-Jones, S., 2014. miRBase: annotating high confidence microRNAs using deep sequencing data. Nucleic Acids Res. 42, D68–D73.
Li, A., Zhang, X.S., Jiang, J.H., Wang, H.H., Liu, X.Q., Pan, Z.G., Zeng, Y.X., 2005. Transcriptional expression of RPMS1 in nasopharyngeal carcinoma and its oncogenic potential. Cell Cycle 4, 304–309.
Li, Z., Huang, C., Bao, C., Chen, L., Lin, M., Wang, X., Zhong, G., Yu, B., Hu, W., Dai, L., Zhu, P., Chang, Z., Wu, Q., Zhao, Y., Jia, Y., Xu, P., Liu, H., Shan, G., 2015. Exon-intron circular RNAs regulate transcription in the nucleus. Nat. Struct. Mol. Biol. 22, 256–264.
Lu, T., Cui, L., Zhou, Y., Zhu, C., Fan, D., Gong, H., Zhao, Q., Zhou, C., Zhao, Y., Lu, D., Luo, J., Wang, Y., Tian, Q., Feng, Q., Huang, T., Han, B., 2015. Transcriptome-wide investigation of circular RNAs in rice. RNA 21, 2076–2087.
Marquitz, A.R., Mathur, A., Edwards, R.H., Raab-Traub, N., 2015. Host gene expression is regulated by two types of noncoding RNAs transcribed from the Epstein-Barr virus *Bam*HI A rightward transcript region. J. Virol. 89, 11256–11268.
Memczak, S., Jens, M., Elefsinioti, A., Torti, F., Krueger, J., Rybak, A., Maier, L., Mackowiak, S.D., Gregersen, L.H., Munschauer, M., Loewer, A., Ziebold, U., Landthaler, M., Kocks, C., le Noble, F., Rajewsky, N., 2013. Circular RNAs are a large class of animal RNAs with regulatory potency. Nature 495, 333–338.
Nigro, J.M., Cho, K.R., Fearon, E.R., Kern, S.E., Ruppert, J.M., Oliner, J.D., Kinzler, K.W., Vogelstein, B., 1991. Scrambled exons. Cell 64, 607–613.
Pfeffer, S., Zavolan, M., Grasser, F.A., Chien, M., Russo, J.J., Ju, J., John, B., Enright, A.J., Marks, D., Sander, C., Tuschl, T., 2004. Identification of virus-encoded microRNAs. Science 304, 734–736.
Pohl, D., Krone, B., Rostasy, K., Kahler, E., Brunner, E., Lehnert, M., Wagner, H.J., Gartner, J., Hanefeld, F., 2006. High seroprevalence of Epstein-Barr virus in children with multiple sclerosis. Neurology 67, 2063–2065.
Rehmsmeier, M., Steffen, P., Hochsmann, M., Giegerich, R., 2004. Fast and effective prediction of microRNA/target duplexes. RNA 10, 1507–1517.
Rickinson, A., Kieff, E., 2007. Epstein-Barr virus. In: Knipe, D., Howley, P. (Eds.), Fields Virology, Fifth ed. Lippincott Williams & Wilkins, Philadelphia, pp. 2655–2700.
Shi, X., Teng, F., 2015. Down-regulated miR-28-5p in human hepatocellular carcinoma correlated with tumor proliferation and migration by targeting insulin-like growth factor-1 (IGF-1). Mol. Cell. Biochem. 408, 283–293.
Taylor, G.S., Long, H.M., Brooks, J.M., Rickinson, A.B., Hislop, A.D., 2015. The immunology of Epstein-Barr virus-induced disease. Annu. Rev. Immunol. 33, 787–821.
Toptan, T., Abere, B., Nalesnik, M.A., Swerdlow, S.H., Ranganathan, S., Lee, N., Shair, K.H., Moore, P.S., Chang, Y., 2018. Circular DNA tumor viruses make circular RNAs. Proc. Natl. Acad. Sci. USA 115, E8737–E8745.
Ungerleider, N., Concha, M., Lin, Z., Roberts, C., Wang, X., Cao, S., Baddoo, M., Moss, W.N., Yu, Y., Seddon, M., Lehman, T., Tibbetts, S., Renne, R., Dong, Y., Flemington, E.K., 2018. The Epstein Barr virus circRNAome. PLoS Pathog. 14, e1007206.
Wang, C., Wu, C., Yang, Q., Ding, M., Zhong, J., Zhang, C.Y., Ge, J., Wang, J., Zhang, C., 2016. miR-28-5p acts as a tumor suppressor in renal cell carcinoma for multiple antitumor effects by targeting RAP1B. Oncotarget 7, 73888–73902.
Wang, F., Flanagan, J., Su, N., Wang, L.C., Bui, S., Nielson, A., Wu, X., Vo, H.T., Ma, X.J., Luo, Y., 2012. RNAscope: a novel in situ RNA analysis platform for formalin-fixed, paraffin-embedded tissues. J. Mol. Diagn. 14, 22–29.
Wang, P.L., Bao, Y., Yee, M.C., Barrett, S.P., Hogan, G.J., Olsen, M.N., Dinneny, J.R., Brown, P.O., Salzman, J., 2014. Circular RNA is expressed across the eukaryotic tree of life. PLoS One 9, e90859.
Young, L.S., Yap, L.F., Murray, P.G., 2016. Epstein-Barr virus: more than 50 years old and still providing surprises. Nat. Rev. Cancer 16, 789–802.
Zhang, Y., Zhang, X.O., Chen, T., Xiang, J.F., Yin, Q.F., Xing, Y.H., Zhu, S., Yang, L., Chen, L.L., 2013. Circular intronic long noncoding RNAs. Mol. Cell 51, 792–806.